

Effective object segmentation based on physical theory in an MR image

Sung-Jong Eun · Hyeonjin Kim · Jung-Wook Park ·
Taeg-Keun Whangbo

Received: 3 February 2014 / Accepted: 8 May 2014 / Published online: 8 June 2014
© Springer Science+Business Media New York 2014

Abstract Object recognition is usually processed based on region segmentation algorithm. Region segmentation in the IT field is carried out by computerized processing of various input information such as brightness, shape, and pattern analysis. If the information mentioned does not make sense, however, many limitations could occur with region segmentation during computer processing. Therefore, this paper suggests effective object segmentation method based on R2 information within the magnetic resonance (MR) theory. In this study, the experiment had been conducted using images including the liver region and by setting up feature points of R2 map as seed points for region growing to enable region segmentation even when the border line was not clear. As a result, an average area difference of 7.5 %, which was higher than the accuracy of conventional region segmentation algorithm, was obtained.

Keywords MR image · Object segmentation · R2 map · SWI · 3D region growing

1 Introduction

Object recognition is a very important part of image processing. It can begin with area segmentation and image segmentation, which is crucial for image interpretation and is an indispensable stage of image processing. Various image segmentation methods have different characteristics and perform differently according to the input image characteristics; but despite these differences, their image segmentation problems have the same causes. According to the

S.-J. Eun · T.-K. Whangbo (✉)
Department of Computer Science, Gachon University, Sujung-Gu, Seongnam, Gyunggi-Do, South Korea
e-mail: tkwhangbo@gachon.ac.kr

S.-J. Eun
e-mail: asclephios@hotmail.com

H. Kim
Department of Medical Sciences, Seoul National University, Jongno-Gu, Seoul, South Korea
e-mail: hyeonjinkim@snu.ac.kr

J.-W. Park
Department of Computer Science, Yonsei University, Seoul, South Korea
e-mail: pjppp@cs.yonsei.ac.kr

distribution of neighboring pixel values, non-segmentation or excessive segmentation occurs. These problems are common chronic problems with various image segmentation methods, and many studies have been conducted to resolve them.

Generally, image segmentation algorithms include the threshold value technique, the edge detection technique, region growing, and the technique of using texture characteristic values [2, 18, 21, 31]. The threshold value method involves creating histograms for the given image, determining the critical value, and partitioning the image into the object and the background. Edge detection refers to the process of looking for gray-level discontinuous pixels in an image. Region growing [27] was designed to measure similarities between pixels to be able to expand and segment an area. In addition, the statistical method and the structural method use texture characteristic values that quantify discontinuous changes in pixel values in an image [39]. In addition to these general methods, methods of segmenting an area manually have been extensively studied, and multi-area segmentation methods are being applied [26]. Of these methods, the Graph Cut [41] method and the GrabCut [35] method of looking for borders to minimize energy have been proposed as methods of minimizing the involvement of users, but they have the disadvantage of requiring the setting of the initial area. Also, the Region Adaptive Algorithm method of extracting features by area using appropriate methods has been proposed, but it has the weakness of yielding inaccurate results in ambiguous borders. To resolve these shortcomings, the curve fitting method based on regional minimum values is being used. In addition, ACM or the snake method [22] was proposed to converge to the point where the energy value is minimum, to detect the optimal contour line. This snake method requires significant user information involvement, however, and has the problem of the misconception of the energy value in a shady area as a different area. To resolve these problems, diverse snake methods have been proposed [10, 20].

Representative image segmentation algorithm stems from the difference in pixel information. The difference in pixel, which is input information, is determined by the difference in brightness or shape/pattern, which is connecting information. However, if the difference cannot be identified from the input information, the accuracy of region segmentation dramatically decreases. This paper suggests an effective segmentation method using magnetic resonance (MR) theory to resolve this problem. Magnetic resonance imaging (MRI) is an examination method that produces images using nuclear magnetic resonance (NMR). Resonance means an amplification reaction to the stimulations having with the same frequencies. NMR method measures the signals that come out from a nucleus when it is stimulated by its own characteristic frequency. Human bodies become feeble magnets in a magnetic field. Because the degree of magnetization differs according to the tissues of a human body, an MRI image can be obtained by measuring and graphing the difference through computer processing [36].

There are three types of MRI images: proton density image, T1 image, and T2 image [7, 8]. This paper worked towards improving the quality of an image including the liver region, and tried to isolate the liver region from the image using three-dimensional region growing method by setting up several feature points of the image as seed points. This method does not use the conventional pixel information for input information, but instead uses R2 map [29].

2 Proposed method

Recognizing the liver in an MRI image provides important information for deciding on therapy or operation method, as well as identifies diseases in the liver. This paper tries to enhance the accuracy of recognition by using R2 map information. The proposed method works as follows:

First, the R2 map information in T2 image is calculated; second, the calculated feature points of the R2 map are detected; and finally, the liver region is isolated using the 3D region growing method in volume data based on the detected feature points. Figure 1 shows the general algorithm flowchart. Detailed and step-by-step explanation will be given thereafter.

2.1 Calculation of R2 map

Magnetic resonance imaging (MRI) methods are now frequently used for the analysis of the diseased tissue. The methods are based on the fact that the spin lattice, T1, and the spin-spin, T2, relaxation times are different as compared to that of the normal tissue. We mention the theoretical analysis of methods for the quantification of the T2 values on Rat. The images obtained were used to construct the T2 maps using the inversion recovery and the fast spin echo pulse sequences. The inversion time, TI, values during the image acquisition with the inversion recovery pulse sequence and the echo time, TE, using the fast spin echo pulse sequence.

In order to obtain the exact solutions for constructing T2 maps, the signal intensity, SI were calculate the following equation 1 [14, 15, 23].

$$SI = SI_0 \left(\exp(-T_E/T_2) \right) \tag{1}$$

SI0 represents the intensity of the MRI signal corresponding to the proton system in the water pool at equilibrium. And T2 maps were TR/TE : 3,000/2.192 ms, NE(number of echo) : 5, slices number : 25, slice thickness : 1 mm, slice gap : 0 mm respectively. The analyzed regions correspond to 192 × 192 pixels. The above sets of images were also processed to extract the T2 maps calculation by equation 2 [14, 15].

$$T_2 = - \frac{T_E}{\ln \left(\frac{SI(T2W)}{SI(PD)} \right)} \tag{2}$$

By taking a reciprocal of the calculated T2 map (1/T2), the R2 map can be calculated. Usually, T2 value depends on the Fe content. Certainly there may be some individual distinction, but if a tissue contains more Fe, the R2 value increases because the T2 value generally decreases. For this reason, this paper tried to conduct region segmentation using R2 map information in the image which includes the liver region. Figure 2 shows the image of the

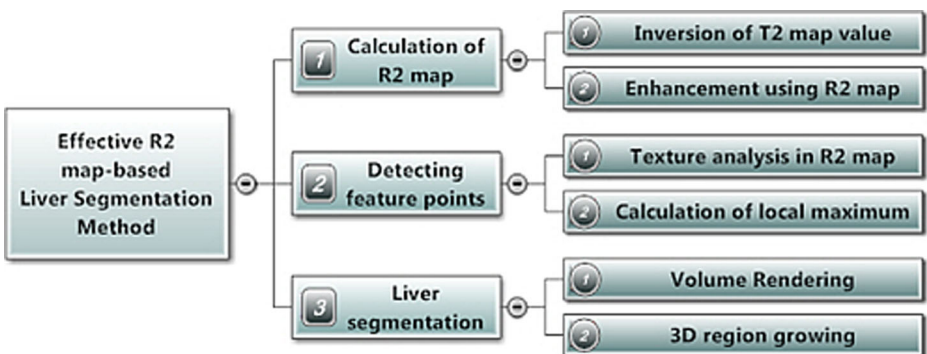


Fig. 1 Overview of the proposed method

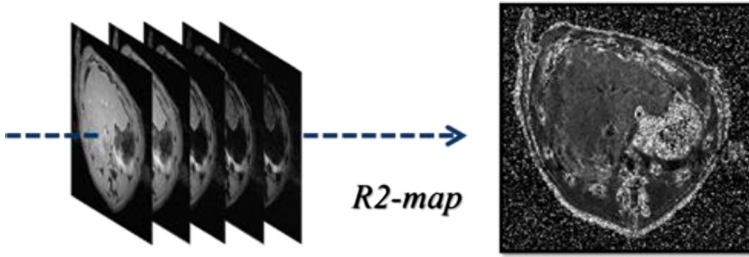


Fig. 2 Result of R2 map Calculation

liver of a rat and illustrates the process results of the R2 map using the equations previously mentioned. Figure 2 also shows that the values calculated near the liver region have meaningful and uniform distribution.

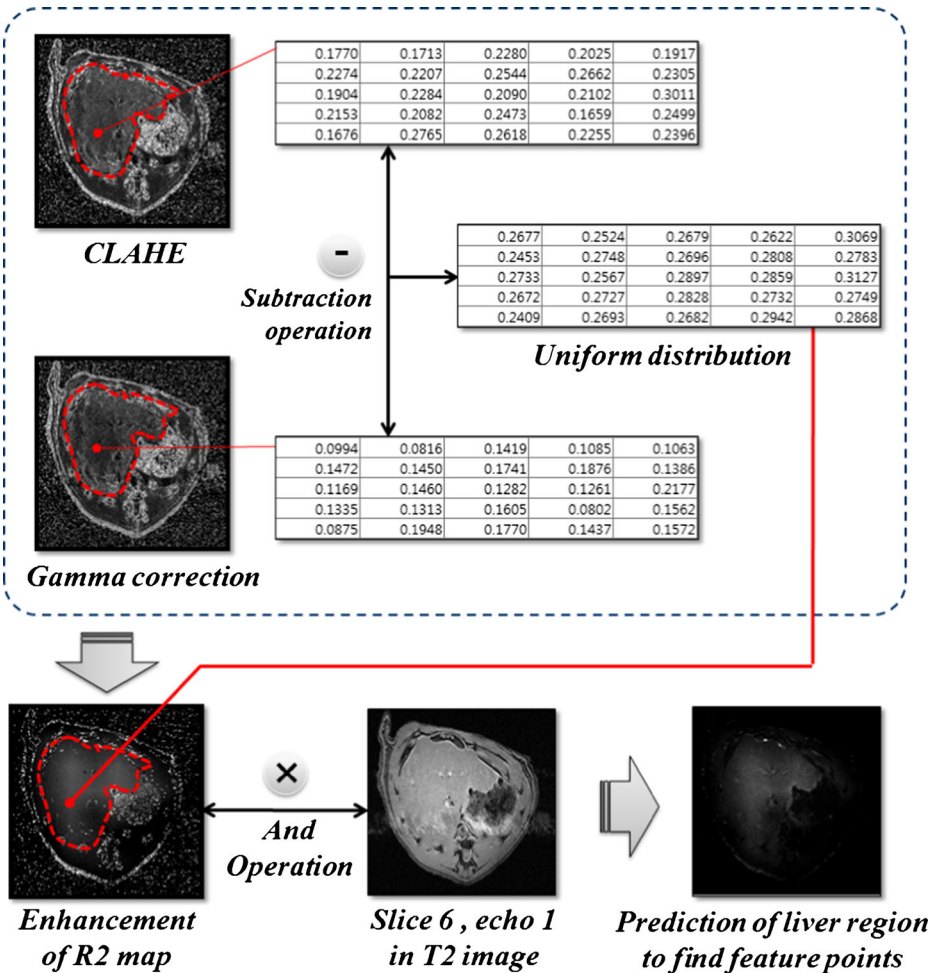


Fig. 3 The enhancement process using R2 map

And we take the enhancement process using R2 map. Next Fig. 3 shows the whole enhancement process using R2 map. According to Fig. 3 process, to enhancement we use the subtraction operation between general gamma correction and CLAHE [30] method. So, we can predict the liver region that uniform distribution by gamma correction and CLAHE method. Because in contrast to gamma correction, CLAHE method can effect to intensity scale factor in widely distribution of intensity. After do enhancement process, we can calculate the meaningful region by AND operation between above enhancement result and input T2 image. So, we can find the feature points in this meaningful region.

2.2 Detecting feature points

In this phase, the feature points of above enhancement result, which have previously been calculated, are detected. The feature points should be set up as seed points in the third phase, which uses the region growing method. Detecting feature points consists of two tasks. First is limiting the scope of detection. This requires establishing a candidate area to detect feature points, within which the actual feature points should be detected. Second is identifying the pixels that are considered meaningful as feature points. These feature points are used as input information of the region segmentation algorithm, which is the next phase.

Deciding on the candidate area for detecting feature points is conducted through texture analysis. The texture analysis in this paper assumes that the candidate area is one that has uniform characteristics when analyzed through co-occurrence matrix [34]. Co-occurrence matrix is one of the tools used in texture imaging and is based on secondary statistical value, which represents the distribution of position pixel values of (x_1, y_1) and (x_2, y_2) . If the dimension of the measured window is $M \times N$ (3×3) and the gray level is L -Level, the dimension of co-occurrence matrix C is $L \times L$, and is calculated as following equation 3.

$$C = \{c_{m,n}\} = C_0 + C_{\pi/2} + C_{\pi} + C_{3\pi/2} \quad (3)$$

$C\theta$ is co-occurrence matrix of a coupled pixel adjacent to θ direction. Co-occurrence matrix is used in detecting the liver region so that a region having homogeneity could be detected in a flexible way. This paper tried to find a region that shows how regularly the brightness of pixels in a window varies using Angular Second Moment (ASM) and Entropy (ENT). Equations 4 can be used in calculating ASM and ENT.

$$ASM : \sum_{i=0}^{N-1} \sum_{j=0}^{N-1} P_{ij}^2 \quad ENT : \sum_{i=0}^{N-1} \sum_{j=0}^{N-1} P_{i,j} (-\ln P_{i,j}) \quad (4)$$

$P_{i,j}$ is used as the weight of each pixel, and it can be said that the bigger the ASM value, the more regularly the brightness changes. The next step is to detect feature points within the candidate liver region. To do so, first we made the binary image through the above enhancement result when we made it, we just using OTSU [1] threshold method. Second, we use the distance transform (DT) [9] in binary image. And third, we do the region growing method by using several seed points that calculate the global maximum value in DT. We set the threshold as average intensity value when we do region growing. So, we can check the widely distribution as candidate liver region. According to this boundary of region, we can find the more meaningful feature points. Figure 4 shows the processing that calculate the candidate liver region to find meaningful feature points.

And we tried to find the feature points using the local maximum value of the pixels in the boundary of region. That Local maximum value based on Harris corner detection [4, 17, 25] method in enhanced image. This method assumes that the feature points show differences in Fe

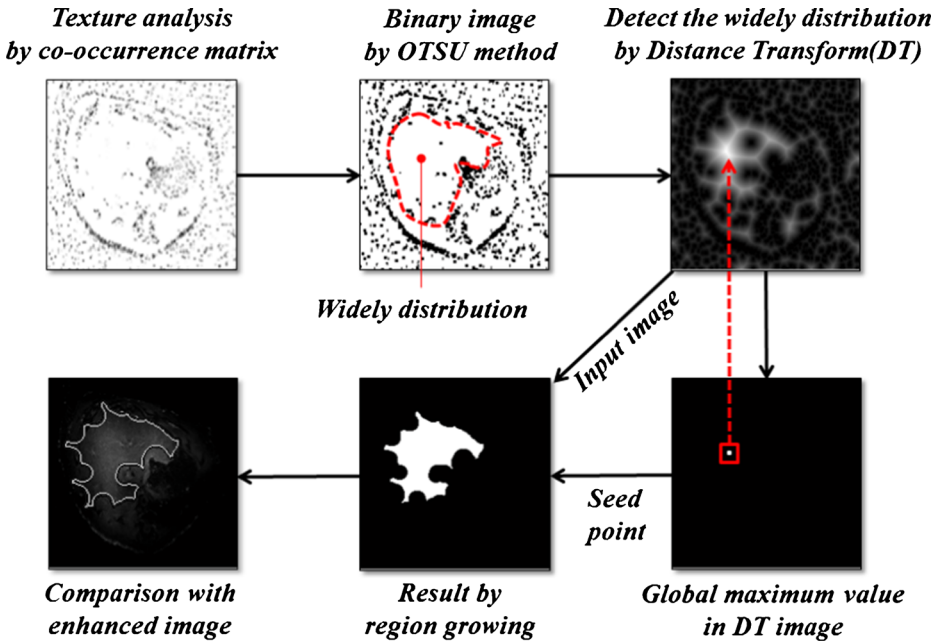


Fig. 4 The Calculation of candidate liver region

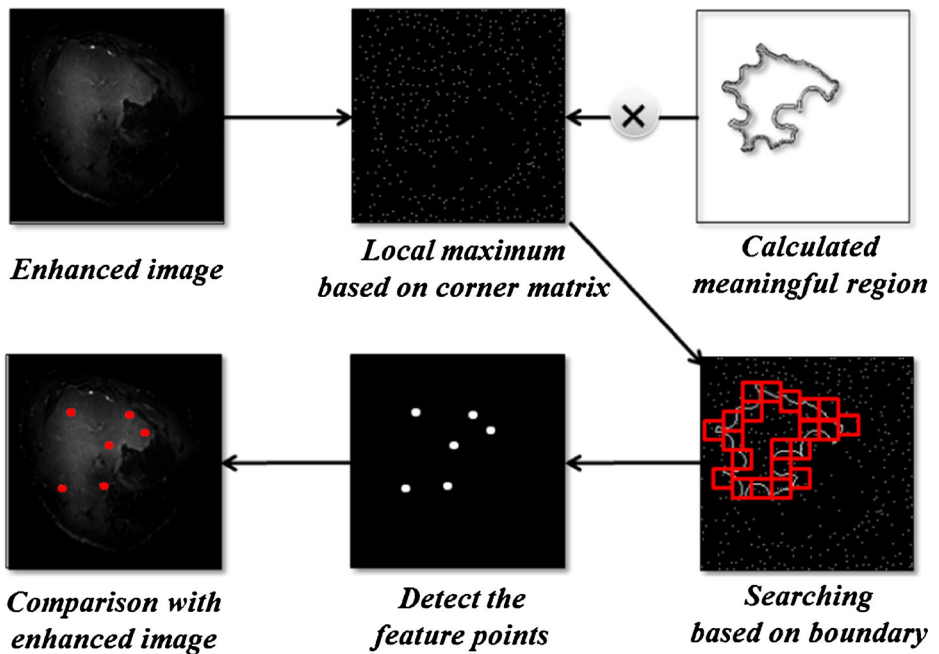


Fig. 5 The final detection of feature points

content in the homogeneous region, and the points can be obtained by local maximum value. This local maximum value can export in compare meaningful boundary with corner matrix. Figure 5 shows the results that were finally detected.

2.3 Liver segmentation

The final phase is to detect the liver region using 3D region growing [3] method with the calculated feature points being set up as seed points. Before using the region growing method, 3D volume data should be created through volume rendering of processed images by Susceptibility Weighted Imaging (SWI). SWI is a new means to enhance contrast in MR imaging [19, 24, 32]. Firstly, all the processing steps involved in the creation of susceptibility weighted magnitude images are schematically summarized in Fig. 6. According to Fig. 6, when we do the phase unwrapping, we choose the 15×15 mask by high-pass filter. And we can get the improved images by SWI process for volume data.

Until recently, with the exception of phase being used for large-vessel flow quantification or for use in inversion recovery sequences, most diagnostic MR imaging relied only on the reading of magnitude information. The phase information was ignored and usually discarded before even reaching the viewing console. Phase images, however, contain a wealth of information about local susceptibility changes between tissues [11, 13, 16], which can be useful in measuring iron content²⁶ and other substances that change the local field. The effects of other background magnetic fields presented a major problem by obscuring the useful phase information. Hence, for nearly 20 years, phase information in flow-compensated sequences went essentially unused as a means to measure susceptibility in clinical MR imaging. And we can make the meaningful volume data of processed result by SWI.

The volume rendering algorithm has two broad types: ray casting and compositing [6, 12, 28, 33, 38]. This paper used ray casting method in creating volume data. In this method, a ray of light is shot to each pixel; and then the value of each voxel, which encounters the light, is projected on the screen; and the color value “ $C(U_i)$,” which corresponds to “ $U_i=(u_i, v_j)$,” is

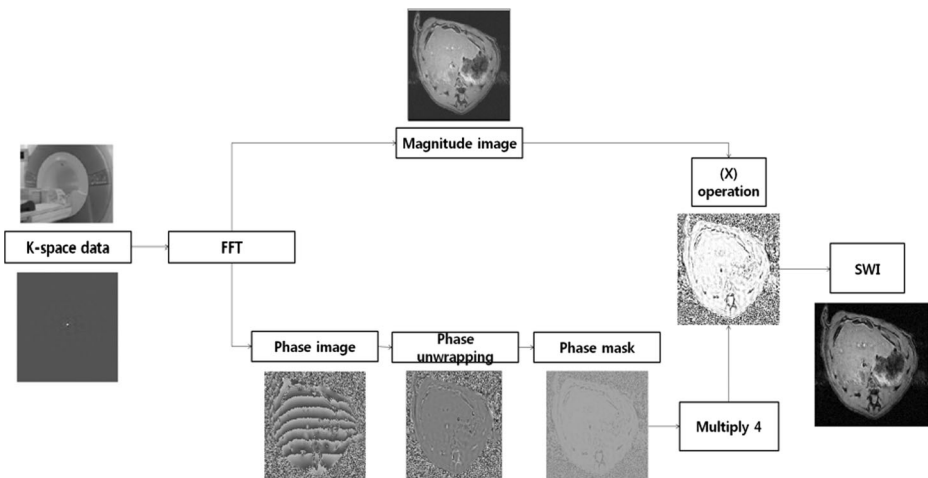


Fig. 6 The whole process of Susceptibility Weighted Imaging (SWI)

obtained by adding the values on the screen using Front to Back method. Equation 5 shows the procedure.

$$C_{out}(U_i) = C_{out}(U_{i-1}) + c(X_i)a(X_i)t(X_{i-1}) \quad (5)$$

In the above equation, $U_i=(u_i, v_j)$ is the position of each pixel; $X_i=(x_i, y_j, z_k)$ is the position of each voxel; $C(U_i)$ is the final color value of each pixel; $c(X_i)$ is re-sampled color value by ray casting; $a(X_i)$ is opacity; and $t(X_i)$ represents the opacity of each voxel from the beginning to the current time. That is, if $t(X_i)=0$, the calculation for one pixel stops and moves to the next one. After that, the color value of the final pixel is decided through the Maximum Intensity Projection (MIP) method [37, 40]. Three-dimensional region growing is processed using the volume data and the calculated feature points. Region growing is an image segmentation method that expands pixels which satisfy homogeneity criterion using the characteristic that the pixels in a region have the same brightness and texture around the initially chosen seed points; and the expanded pixels form a region. Accordingly, in order to expand pixels, appropriate choice of homogeneity criterion is crucial. In this paper, the seed points were decided using the 3D coordinate values of previously calculated feature points. And while expanding voxels, the average brightness of the candidate region obtained through the co-occurrence matrix was established as a threshold. Assuming the possibility of error in that the expansion could include irrelevant voxels, the previously calculated border lines are considered while adjusting the boundary of the region. The task of fitting entails adjusting the border line to the original one if the results of 3D region growing deviate from the border line. And the final post processing is curve fitting that needed to modify the border line. For curve fitting in this step, the boundary is created through the Catmul-Rom spline curve [5]. The boundary is finally determined through template matching. They are symmetrically positioned around the center of gravity of the ROI, and the boundary information is considered instead of the segmentation candidates. This information was used for comparison of the matching information because the target of this method is the segmentation of objects with true circular shapes. Equation 5 below shows this curve-fitting method. Lastly, the boundary is smoothened using a Median filter.

$$Q(t) = 0.5 \times (1.0f, t, t^n) \times [Mat_{n \times n}] \times [P_{n-1}] \quad (6)$$

Given the control points P0, P1, P2, and P3 and the value t, the location of the point can be calculated. P represent the control points, t represent the signifies the portion of the distance between the two nearest control points, Mat represent the nxn matrix. Figure 7 shows modified result by sample slice 1 and 9.

Figure 8 shows the final results of the proposed procedure. In order to check the rotation status in volume liver object, we include the major axis that red color dotted line.

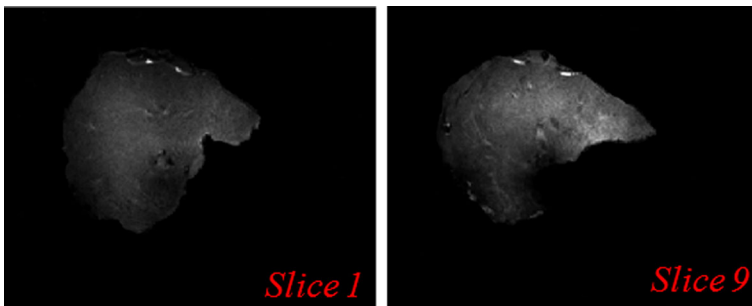


Fig. 7 Sample result of liver segmentation

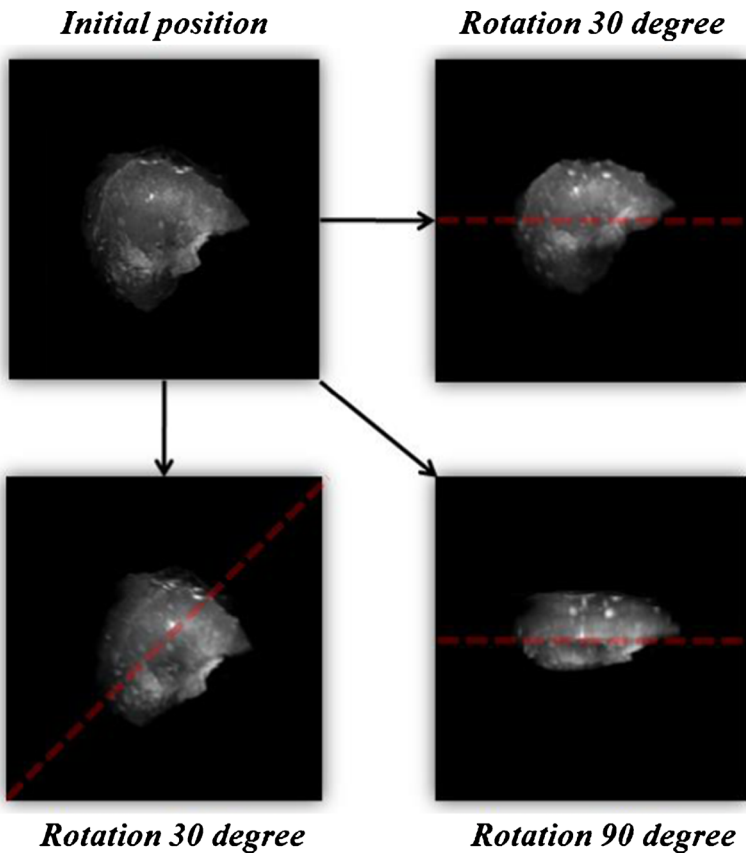


Fig. 8 Final result of liver volume data

3 Experiment

To evaluate the proposed method, experiments based on medical MRI imaging were performed, and the results were compared with the reference image achieved by a specialist doctor. Thus, the accuracy of the method was evaluated quantitatively. Towards this end, the difference ratio between the reference image and the area from the proposed method was calculated, and can be expressed by the following equation.

$$R_{diff} = \frac{|R_{criteria} - R_{proposed}|}{R_{criteria}} \times 100 \quad (7)$$

Table 1 Results of comparison of the proposed method with the other exist methods

Method	Average area difference ratio
Region growing	15.4 %
Snake	10.2 %
Proposed method	7.5 %

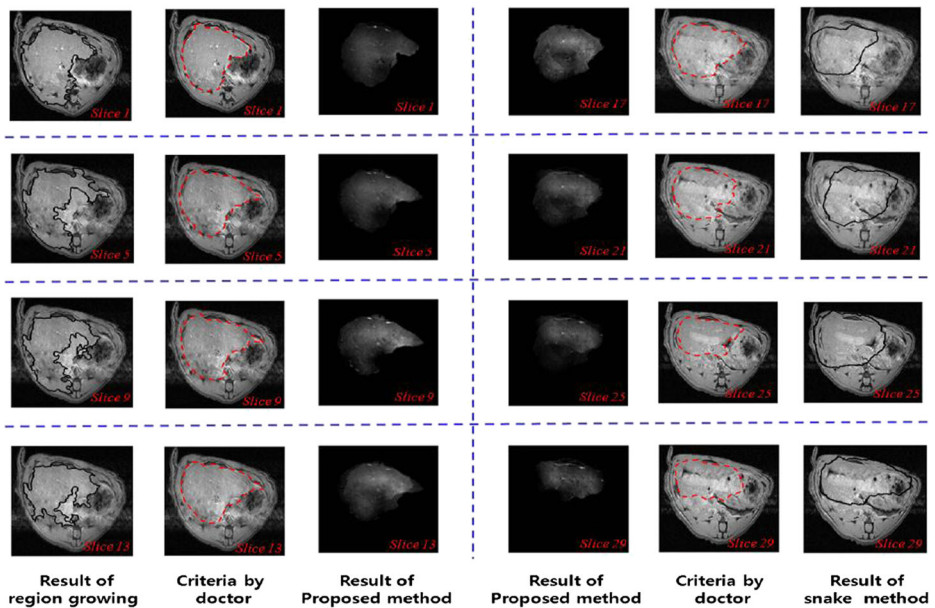


Fig. 9 The results of compare proposed method and exist method

In Equation 7, R_{diff} denotes the area difference ratio, $R_{criteria}$ denotes the area of the reference image, and $R_{proposed}$ represents the area created by the proposed method. For this experiment, a total of 25 MRI images were processed. And the relevant image criteria were evaluated according to the results of the proposed method and of Equation 7, after a specialist doctor established the baseline using Adobe Photoshop CS. In our case, to evaluate the accuracy, we calculate the average area difference by each slice in liver volume object. As a result, an average area difference ratio of 7.5 % was determined. Table 1 show the results of the application of the comparison algorithm.

Actually, proposed method is composed of general segmentation algorithm in addition to MR theory as R2 map information. So that's why we choose the comparison method like a region growing and snake model. In case of region growing, seed point is set the manually by criteria boundary. Threshold value was calculated by average intensity. In case of snake model, initial contour set the manually by criteria boundary. According to the results shown in Fig. 9 and Table 1, the existing region growing and snake method caused some problems in that the intensity or energy recognized portions with ambiguous shades as different areas.

4 Conclusion

In this paper, R2 map information within the MR theory has been used to resolve the basic limitations in computer processing. It suggested detection of meaningful feature points. It also suggested an effective algorithm to detect the liver region using 3D region growing based on feature points. This method did not stick to fundamental brightness processing, but focused on finding the region that contains high Fe content through R2 map calculation, considering the functional characteristics of the liver region. The results have confirmed that the feature points, which have been detected through a corresponding R2 map, are meaningful; that is, the method

in which the feature points detected through R2 map were used was more accurate than the conventional one in which the difference of pixel information was used. However, when the R2 map has considerable noise or has been distorted from the original gray image, the accuracy of detection becomes low. This limitation should be complemented by further research on image improvement. This paper aimed to verify the possibility of improvement in computer processing by adopting the MR theory. Further research needs to be conducted to help in resolving the general limitations through the appropriate combination of MR theory and computer science.

Acknowledgments This research was supported by MSIP (the Ministry of Science, ICT and Future Planning), Korea, under the IT-CRSP (IT Convergence Research Support Program) (NIPA-2013-H0401-13-1001), supervised by the NIPA (National IT Industry Promotion Agency); and by a grant from the Korea Healthcare Technology R&D Project of the Ministry of Health and Wealth of the Republic of Korea (A080369).

References

1. Arie Kaufman (1991) "Introduction to Volume Visualization.," A. Kaufman(ed.), Computer Society Press
2. Baba N, Ichse N, Tanaka T (1996) Image area extraction of biological objects from a thin section image by statistical texture analysis. *Electron Microscop* 45:298–306
3. Bhalla M, Naidich DP, McGuinness G, Gruden JF, Leitman BS, McCauley DI (1996) Diffuse lung disease : assessment with helical CT -preliminary observations of the role of maximum and minimum intensity projection images. *Radiology* 200:341–347
4. Calhoun PS, Kuszyk BS, Heath DG, Carley JC, Fishman EK (1999) Three-dimensional volume rendering of spiral CT data : theory and method. *RadioGraphics* 19:745–764
5. Catmull E, Rom R (1974) "A class of local interpolating splines.," *Computer Aided Geometric Design*, pp.317–326
6. Chande B, Dutta Majumder D (1988) "A note on the graylevel co-occurrence matrix in threshold selection", *Signal Processing*, 15(2)
7. Damadian RV (1971) *Science* 171:1151–1153
8. de Graaf RA, Brown PB, McIntyre S, Nixon TW, Behar KL, Rothman DL (2006) *Magn Reson Med* 56:386–394
9. Drebin RA, Carpenter L, Hanrahan P (1988) Volume rendering. *Comput Graph* 22(4):65–74
10. Eddie Y, Ng K, Chen Y (2006) Segmentation of the breast thermogram: improved boundary detection with the modified snake algorithm. *J Mech Med Biol* 6(2):123–136
11. Fernandez-Seara MA, Techawiboonwong A, Detre JA et al (2006) MR susceptometry for measuring global brain oxygen extraction. *Magn Reson Med* 55:967.73
12. Gavrilu DM, Daimler-Benz AG (1998) "Multi-feature Hierarchical Template Matching Using Distance Transforms", *IEEE International Conference on Pattern Recognition*
13. Haacke EM, Ayaz M, Khan A et al (2007) Establishing a baseline phase behavior in magnetic resonance imaging to determine normal vs abnormal iron content in the brain. *J Magn Reson Imaging* 26:256.64
14. Haacke EM, Brown RW, Thompson MR, Venkatesan R (1999) *Magnetic resonance imaging:physical principles and sequence design*. Wiley, USA, pp 129–133
15. Haacke EM, Brown RW, Thompson MR, Venkatesan R (1999) *Magnetic resonance imaging:physical principles and sequence design*. Wiley, USA, pp 118–123
16. Haacke EM, Lai S, Reichenbach JR et al (1997) In vivo measurement of blood oxygen saturation using magnetic resonance imaging: a direct validation of the blood oxygen level-dependent concept in functional brain imaging. *Human Brain Mapp* 5:341–46
17. Hanrahan P (1990) Three-pass affine transforms for volume rendering. *Computer Graph* 24(5):71–78
18. Hemachande S, Verma A, Arora S, Panigrahi PK (2007) Locally adaptive block thresholding method with continuity constraint. *Pattern Recogn Lett* 28:119–124
19. Hu J, Yu Y, Juhasz C et al (2008) MRsusceptibility weighted imaging (SWI) complements conventional contrast enhanced T1 weighted MRI in characterizing brain abnormalities of Sturge-Weber syndrome. *J Magn Reson Imaging* 28:300.07
20. Kang DJ, In Kweon S (1999) A fast and stable snake algorithm for medical images. *Pattern Recogn Lett* 20(10):1069
21. Kang CC, Wang WJ (2007) A novel edge detection method based on maximization of the objective function. *Pattern Recogn* 40(2):609–618
22. Kass M, Witkin A (1988) Demeter terzopoulos active contour models. *Int J Comput Vis* 1:321–331
23. Kingsley PB (1999) *Concepts in Magn Reson* 11:29–49

24. Koopmans PJ, Manniesing R, Niessen WJ, et al. (2008) MR venography of the human brain using susceptibility weighted imaging at very high field strength. *MAGMA* 21:149–58. Epub 2008 Jan 11
25. Levoy M (1988) Volume rendering, display of surface from volume data. *IEEE Comput Graph Appl* 8(5):29–37
26. Li W, Zhou C, Zhang Z (2004) Segmentation of the body of the tongue based on the improved snake algorithm in traditional Chinese medicine. In Proc. of the 5th World Congress on Intelligent Control and Automation, pp. 15–19
27. Muerle JL, Allen DC (1968) Experimental evaluation of a technique for automatic segmentation of objects in complex scenes. *IPPR*, Thompson
28. Otsu N (1979) A thresholding selection method from gray-scale histogram. In *IEEE Transactions on System, Man, and Cybernetics* 9(1):62–66
29. Pippa Storey, PhD, Alexis A. Thompson, Christine L. Carqueville, BA, John C. Wood, R. Andrew de Freitas, and Cynthia K. Rigsby (2007) R2* Imaging of Transfusional Iron Burden at 3T and Comparison with 1.5T. *J Magn Reson Imaging* 25, pp.540–547
30. Pizer SM, Johnston RE, Ericksen JP, Yankaskas BC, Muller KE (1990) “Contrast-limited adaptive histogram equalization: speed and effectiveness,” *Visualization in Biomedical Computing*, pp.337-345
31. Rafael C. Gonzalez and Paul Wintz (1993) *Digital Image Processing*, 3rd Ed., Addison-Wesley
32. Reichenbach JR, Venkatesan R, Schillinger DJ et al (1997) Small vessels in the human brain: MR venography with deoxyhemoglobin as an intrinsic contrast agent. *Radiology* 204:272–77
33. Remy-Jardin M, Remy J, Artaud D, Deschildre F, Duhamel A (1996) Diffuse infiltrative lung disease : Clinical value of sliding-thin-slab maximum intensity projection CT scans in the detection of mild micronodular patterns. *Radiology* 200:333–339
34. Rose J-L, Revol-Muller C, Almajdub M, Chereul E, Odet C (2007) “Shape prior integrated in an automated 3d region growing method,” in *Image Processing, 2007. ICIP 2007. IEEE International Conference on*, vol. 1, pp. 53–56
35. Rother C, Kolmogorov V, Blake A (2004) GrabCut: Interactive foreground extraction using iterated graph cuts. *ACM Trans Graph* 23(3):309–314
36. Shrager RI, Weiss GH, Spence RGS (1998) *NMR Biomed* 11:297–305
37. Thomas M. Murphy, Mark Math, and Leif H. Finkel (2003) “Curvature Covariation as a Factor of Perceptual Saliency,” *International IEEE EMBS CNECI*, pp. 16–19
38. Umut Orguner, Fredrik Gustafsson (2007) “Statistical Characteristics of Harris Corner Detector”, *IEEE/SP 14th Workshop*, pp.571-575
39. Unser M (1995) Texture classification and segmentation for using wavelet frames. *IEEE Trans* 4(11):1549–1560
40. Williams D, Shah M (1992) A fast algorithm for active contours and curvature estimation. *Comput Vis Graph Image Process: Image Underst* 55:14–25
41. Zabih R, Kolmogorov V (2004) Spatially coherent clustering using graph cuts. In *Proc Comput Vision Pattern Recognit* 2:437–444



Sung-Jong Eun received the M.S. degree from Gachon University of South Korea in 2009 and the Ph. D candidate both in Computer Science from Gachon University in 2012. His research areas include Computer Graphics, Medical image processing, BCI, AR.



Hyeonjin Kim received his M.S. degree in Physics from Polytechnic University, Brooklyn, NY, USA in 1996 and Ph. D degree in Biomedical Engineering from University of Alberta, Edmonton, AB, Canada. Currently, his research is focused on developing magnetic resonance imaging and spectroscopy techniques for the diagnosis of liver diseases.



Jung-Wook Park received the BS, MS, and the Ph.D. degrees in computer science from Yonsei University, Seoul, Korea in 2003, 2005, and 2010. Currently he carries out research about memory hierarchy optimization for various computer systems and software/hardware co-design for embedded parallel systems.



Taeg Keun Whangbo received the M.S. degree from City University of New York in 1988 and the PhD degree both in Computer Science from Stevens Institute of Technology in 1995. Currently, he is a professor in the Department of Interactive Media, Gachon University, Korea. He is also the Dean of Research Affairs in Gachon University. Before he joined the Gachon University, he was the software developer in Q-Systems which is located in New Jersey from 1988 to 1993. He was also the researcher in Samsung Electronics from 2005 to 2007. From 2006 to 2008, he was the president of the Association of Korea Cultural Technology. His research areas include Computer Graphics, HCI and AR.